

Quantum Phases of Cold Polar Molecules in 2D Optical Lattices

B. Capogrosso-Sansone,¹ C. Trefzger,² M. Lewenstein,² P. Zoller,³ and G. Pupillo³

¹ITAMP, Harvard-Smithsonian Center of Astrophysics, Cambridge, MA, 02138, USA

²ICREA and ICFO - Institut de Ciències Fotoniques, 08860 Castelldefels (Barcelona), Spain

³IQOQI and Institute for Theoretical Physics, University of Innsbruck, 6020 Innsbruck, Austria

We discuss the quantum phases of hard-core bosons on a two-dimensional square lattice interacting via repulsive dipole-dipole interactions, as realizable with polar molecules trapped in optical lattices. In the limit of small tunneling, we find evidence for a devil's staircase, where solid phases appear at all rational fillings of the underlying lattice. For finite tunneling, we establish the existence of extended regions of parameters where the groundstate is a supersolid, obtained by doping the solids either with particles or vacancies. Here the solid-superfluid quantum melting transition consists of two consecutive second-order transitions, with a supersolid as the intermediate phase. The effects of finite temperature and confining potentials relevant to experiments are discussed.

PACS numbers: 03.75.-b, 05.30.-d, 67.85.-d, 67.80.-kb

Atomic physics experiments with quantum degenerate gases are establishing themselves as a quantitative tool to measure the phase diagram of complex many body systems [1]. A prime example is the superfluid - Mott insulator quantum phase transition with cold bosonic atoms in optical lattices representing a Bose Hubbard model with onsite interactions [2, 3]. Recent experiments have provided increasingly quantitative studies of these quantum phases in excellent agreement with Quantum Monte Carlo calculations [4]. The challenge is now to extend these quantitative comparisons to a broader class of Hubbard models, as part of a program to develop optical lattice emulators for many body systems. Of particular interest is the role of offsite interactions in Hubbard models [5], which are strongly suppressed for atoms due to the short range character of the interactions. The recent breakthrough in preparing cold ensembles of polar molecules [6] has opened the door, however, to a study of dipolar quantum gases with long range interactions [5, 7]. In particular, bosonic polar molecules on a 2D lattice provide a realization of Hubbard-like models for *hard-core* particles with *long-range interactions* [9]. In the present work we will show that this model displays novel quantum phenomena which have no counterpart in the atomic case. These include: (i) a devil's staircase of Mott lobes at rational lattice fillings, (ii) supersolid phases by doping solids with either vacancies or additional particles. We find that the long-range interactions stabilize the supersolid as the low-energy phase for a large range of system's parameters, raising interesting prospects for the realization of this exotic phase with polar molecules in optical lattices.

In the following, we consider a setup where N bosonic polar molecules are confined to a 2D plane by a strong transverse trapping field, e.g a 1D optical lattice, and are aligned perpendicular to the plane, with a DC induced dipole moment $d = \sqrt{D}$ [8]. An additional 2D optical lattice confines the particles in-plane. Combined with the requirement that the initial system has no

doubly occupied sites, this realizes the following Hamiltonian for hard-core bosons on a 2D square lattice [9]

$$H = -J \sum_{\langle i,j \rangle} [b_i^\dagger b_j + b_i b_j^\dagger] + V \sum_{i < j} \frac{n_i n_j}{r_{ij}^3} - \sum_i \mu_i n_i. \quad (1)$$

The first and second terms in Eq. (1) describe the standard kinetic energy with hopping rate J and the repulsive dipole-dipole interaction with strength $V = D/a^3$ with a the lattice spacing and $r_{ij} = |i - j|$, respectively; b_i and b_i^\dagger are bosonic operators with $b_i^{\dagger 2} = 0$ and $n_i = b_i^\dagger b_i$; $\mu_i = \mu - \Omega i^2$, with μ the chemical potential and Ω the curvature of an external harmonic confinement. We have studied the quantum phases of Eq. (1) by means of large scale Monte-Carlo simulations based on the Worm Al-

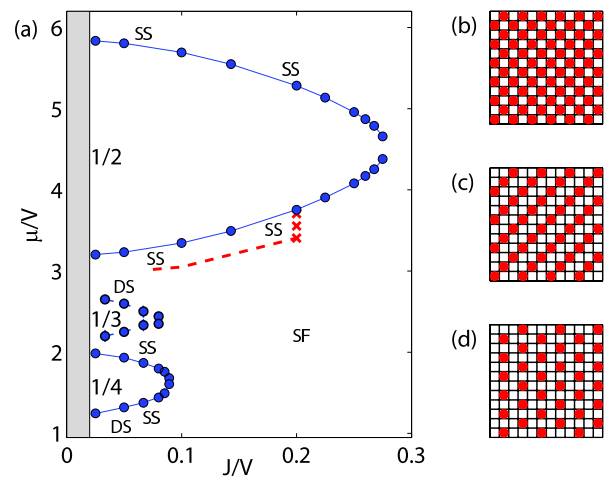


FIG. 1: (color online) (a) Phase diagram of Eq. (1) as a function of μ and J at zero temperature. Lobes: Mott solids (densities indicated); SS: supersolid phase; SF: superfluid phase. DS: parameter region where devil's staircase is observed. Red crosses: width of the SS phase for $J/V = 0.2$ (see Fig. 3). Dashed line: sketch of the SS/SF boundary (see text). Panels (b-d): sketches of the groundstate configuration for the Mott solids in panel (a), with $\rho = 1/2, 1/3$ and $1/4$, respectively.

gorithm [10], using no cutoff in the range of the dipole-dipole interaction [11]. In the following, we start with a brief overview of the basic features, followed by a more detailed discussion of the results.

Homogeneous case, i.e. $\Omega = 0$: Our main results are summarized in Fig. 1(a), the computed zero-temperature phase-diagram as a function of μ and J , in the range $1 < \mu/V < 6$ and $J/V > 0.02$ (unshaded area). We find:

i) Incompressible phases. We have focused on solid phases at rational filling factors $\rho = 1/2, 1/3$, and $1/4$, (Mott lobes in Fig. 1). The corresponding groundstate configurations are sketched in panels (b-d). Mott lobes at other rational filling factors, e.g. $\rho = 1$, $\rho = 7/24$, are not shown here. We find that for small-enough hopping $J/V \ll 0.1$ the low-energy phase is incompressible ($\partial\rho/\partial\mu = 0$) for most values of μ , and displays a large number of low-energy metastable states. The corresponding parameter region is labeled as DS in the figure. The latter has no analogue for short-range interactions, and is reminiscent of the classical *devil's staircase*, i.e. a succession of incompressible ground states, dense in the interval $0 < \rho < 1$, with a spatial structure commensurate with the lattice for all rational fillings [12].

ii) Supersolid phases. For large enough J/V , the low-energy phase is superfluid (SF), for all μ . At intermediate values of J/V , however, we find that by doping the Mott solids *either with vacancies* (removing particles) *or interstitials* (adding extra particles) a supersolid phase (SS) can be stabilized, with coexisting superfluid and crystalline orders (we find no evidence of SS in the absence of doping). While recent theoretical studies have established the existence of SS phases for bosons on a 2D lattice with nearest-neighbor and next-nearest-neighbor interactions [14, 15], here we address the fundamental question of the emergence of SS behavior in a system with long-range interactions. We show evidence that the solid/superfluid transition consists of a two-step transition, with both transitions of the second-order and the supersolid as the intermediate phase (see Fig. 3 below).

iii) Finite temperature. For experiments, a fundamental question is the observability of the phases described above for finite temperature T . In particular, for the SS phase we show below in Fig. 4 that by increasing T it melts into a featureless normal fluid via a two-step transition, the intermediate phase being a normal fluid with finite density modulations, similar to a liquid crystal.

Harmonic trap, i.e. $\Omega \neq 0$: Assuming local density approximation, an external harmonic potential provides a sweep in chemical potential at constant J/V in the phase diagram of Fig. 1. This results in a shell structure with alternating Mott solids with rational lattice fillings, SS, and SF phases, analogous to the Mott shells with contact interactions [2, 3, 16]. However, we find that finite temperature and the presence of several low-energy metastable states can introduce extended defects in this

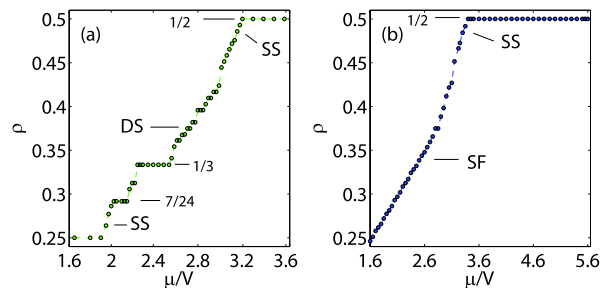


FIG. 2: (color online) ρ vs. μ . (a): Solids and SS for a system with linear size $L = 12$ and $J/V = 0.05$. Some ρ are indicated. (b): SF and vacancy-SS for $L = 16$ and $J/V = 0.1$.

structure [see Fig. 5]. We show that the phases above can be realized with polar molecules of current experimental interest. We refer to Ref. [17] for a study in 1D.

Incompressible phases: The groundstates of the Mott lobes at $\rho = 1/2, 1/3$, and $1/4$ are found to be checkerboard (CB), stripe (ST), and star (SR) solids, respectively [see Fig. 1(b-d)]. For each Mott lobe, the solid order is characterized by a finite value of the structure factor $S(\mathbf{k}) = \sum_{\mathbf{r}, \mathbf{r}'} \exp[i\mathbf{k}(\mathbf{r} - \mathbf{r}')] \langle n_{\mathbf{r}} n_{\mathbf{r}'} \rangle / N$, with \mathbf{k} the reciprocal lattice vector for each solid. For the CB, ST, SR solids, this is (π, π) , $(\pm 2\pi/3, 2\pi/3)$, and $(\pi, 0)$ [or $(0, \pi)$], respectively. The boundaries of the Mott lobes have been calculated from the zero momentum Green function (see e.g. [18]), for linear system sizes up to $L = 20$ (CB and SR lobes), and from $\rho(\mu)$ -curves with sizes up to $L = 24$ (ST lobe). As expected, we find that the CB solid is the most robust against hopping and doping, and thus it extends furthest in the μ - J plane.

Interestingly, we find evidence for incompressible phases in addition to those corresponding to the lobes in Fig. 1. This is shown in Fig. 2, where the particle density ρ is plotted as a function of the chemical potential μ for $J/V = 0.05$, and 0.1 [panels (a) and (b), respectively]. In the figure, a continuous increase of ρ as a function of μ signals a compressible phase, while a solid phase is characterized by a constant ρ for increasing μ . Panel (a), corresponding to $J/V = 0.05$, shows a series of large constant-density plateaux connected by a progression of smaller steps and regions of continuous increase of ρ . Here, the main plateaux correspond to the Mott lobes of Fig. 1, while the other steps correspond to incompressible phases, with a fixed, *integer*, number of particles. We interpret this progression of steps as an indication of a devil's-like staircase in the density, the latter being fully realized in the classical limit of zero hopping.

Since the simulations are necessarily performed for finite L (with periodic boundary conditions) and T , only the lobes with comparatively short periodicity (e.g., $\rho = 1/2$ and $1/4$) and sizeable gaps will be resolved in the calculations. Consistently, we find that determining the

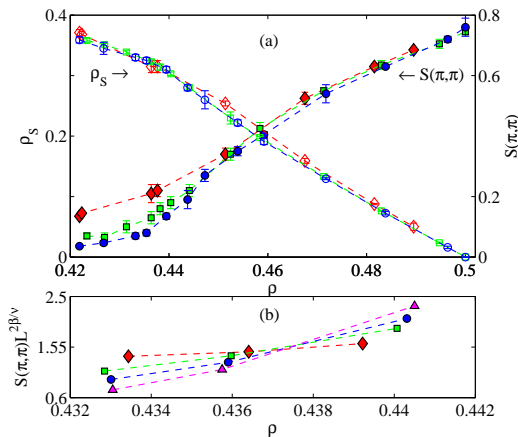


FIG. 3: (color online) Vacancy supersolid for $J/V = 0.2$: (a) ρ_s (empty symbols) and $S(\pi, \pi)$ (full symbols) vs. ρ , for $L = 8, 12, 16$ and 20 (diamonds, squares, dots, and triangles, respectively); (b) $S(\mathbf{k})L^{2\beta/\nu}$ vs. ρ , with $2\beta/\nu = 15/16$. The crossing indicates an Ising-type second-order transition.

groundstate configuration for each DS-step directly from the simulation is often challenging, since: *i*) for many rational fillings [e.g. $\rho = 7/24$ in panel (a)] it would require to consider system sizes (much) larger than those considered here, and *ii*) the long-range interactions determine the presence of numerous low-energy *metastable* states [19], which for finite T can result in the presence of defects or in disordered structures. For example, for $\rho \simeq 0.4$ (below the CB lobe) we have performed simulations with up to $L = 60$ sites and temperatures as low as $T = 0.03125J$. We observe that the groundstate configuration is made of small CB domains separated by quasi-one-dimensional defects. While the latter seem to form a network, it is very difficult to establish whether an ordered ‘superstructure’ may exist in the thermodynamic limit, or whether this apparently disordered phase persists. By measuring the superfluid stiffness $\rho_s = T\langle W^2 \rangle$, with W the winding number, we find no evidence of superfluidity. However, we note that the practical relevance of these Mott lobes with large periodicity is somewhat limited, since they will most likely *not* be observable in experiments with trapped molecules (see below).

Supersolid phases: A very different situation is shown by the behavior of $\rho(\mu)$ immediately above the SR plateau of panel (a), and below the CB plateau of panel (b) in Fig. 2. Here the density grows smoothly with increasing μ , signaling a fluid phase, and we find that ρ_s is finite. Remarkably, and in contrast to previous studies with shorter-range interactions, we find that the appropriate structure factor $S(\mathbf{k})$ corresponding to these solid remains finite for chemical potentials μ below and above each Mott lobe, signaling the existence of both vacancy-induced and particle-induced supersolidity, with no indication of phase-separation. We measured su-

persolid behavior around both Mott lobes with $\rho = 1/2$ and $1/4$, for $J/V \gtrsim 0.05$ and 0.067 , respectively. As an example, Fig. 3(a) shows the case of vacancy-induced supersolidity for $J/V = 0.2$, and $L = 8, 12, 16$ and 20 (red diamonds, green squares, blue circles, and purple triangles, respectively). The figure shows that for an extended range of densities, both the superfluid stiffness ρ_s and the static structure factor $S(\pi, \pi)$, are finite and size-independent, signaling a supersolid. We find evidence that the SS melts into a superfluid via a second-order Ising-type quantum phase-transition. This is shown by the crossing of the curves in panel (b) of Fig. 3, where we plot $S(\mathbf{k})L^{2\beta/\nu}$ as a function of density (the critical exponents $2\beta/\nu = 15/16$ correspond to the three-dimensional Ising universality class). We find that the supersolid behavior persists for smaller J/V -ratios, however the superfluid stiffness tends to decrease with J/V . It remains an interesting question to study the merging of the supersolid phase into the incompressible, disordered, phase described above for small J/V . While the results above point to a generic mechanism for solid/liquid transitions in 2D with the SS as the intermediate phase [20], we have not found evidence of SS or SF phases below and above the ST lobe. This may be due to an extremely low T for superfluidity (here we have used $T_{\min} = J/3L$) or to the existence of an intermediate ‘micro-emulsion’ phase [21].

Finite-T: We studied the melting of the supersolid into a normal phase with increasing T , for the case of vacancy supersolidity below the CB solid, with $J/V = 0.1$. Figure 4 shows ρ_s and $S(\pi, \pi)$ vs T . We find that the melting of the supersolid proceeds through two successive transitions. First, the supersolid melts into a liquid-like

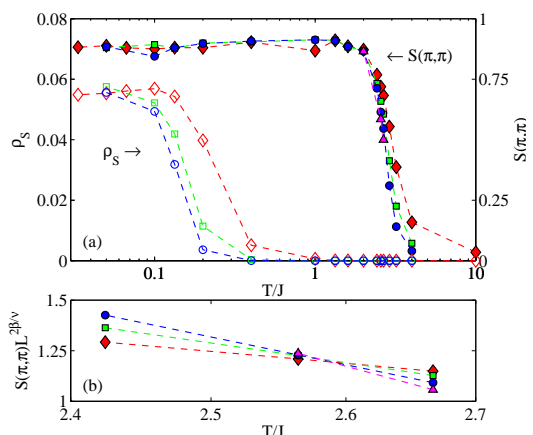


FIG. 4: (color online) Finite- T melting of SS at $J/V = 0.1$: (a) ρ_s (empty symbols) and $S(\pi, \pi)$ (full symbols) vs. T , for $L = 8, 12, 16$ and 20 (diamonds, squares, dots, and triangles, respectively); (b) $S(\mathbf{k})L^{2\beta/\nu}$ vs. T , with $2\beta/\nu = 1/4$.

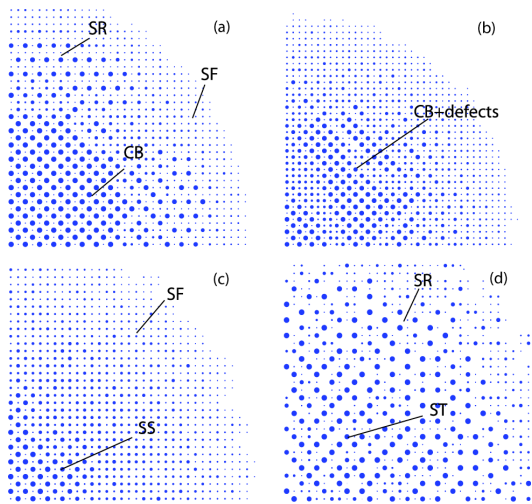


FIG. 5: (color online) Spatial density profile in 2D for $N \simeq 1000$ particles in a harmonic potential (see text). Phases are indicated. (a-b) $V/J = 15$, $\mu/J = 55$, $\Omega/J = 0.05$ and $T/J = 0.0377$; (c) $V/J = 5$, $\mu/J = 19$, $\Omega/J = 0.01$ and $T/J = 0.1$; (d) $V/J = 20$, $\mu/J = 51$, $\Omega/J = 0.04$ and $T/J = 0.25$.

phase reminiscent of a liquid crystal, with zero ρ_s and finite $S(\pi, \pi)$. The drop of ρ_s for $T \simeq 0.1J$ in Fig. 4 signals a transition of the Kosterlitz-Thouless (KT) type, with critical melting temperature $T_{KT} = \pi \rho_s \hbar^2 \rho / 2m$, and $m = 1/2Ja^2$. Upon further increasing temperature, we find that the static structure factor drops to zero for $T \simeq J = 0.1V$. In panel (b) we show that this is consistent with an Ising-type transition, by plotting the expected scaling for $S(\pi, \pi)$ in two dimensions (here, $2\beta v = 1/4$). Thus, we find that in this case the supersolid melts into a featureless normal fluid via a two-step transition, where the intermediate phase retains solid-like, but not superfluid-like, order, reminiscent of liquid crystals. The KT- and Ising-type scalings allow for the estimation of the critical melting temperatures for various system parameters (e.g., $T_{KT} \simeq 0.3J$ for Fig. 3).

Harmonic trap: Experiments will be performed in harmonic traps, producing a wedding-cake structure in the density profile. This may provide for, e.g., a direct realization of DS in a single experiment. In order to show what experiments will realize, we have performed simulations with a harmonic potential of curvature Ω , for experimentally relevant systems with $N \simeq 1000$ particles and finite T . In Fig. 5 we show maps of the spatial density distribution in the lattice (shown is a single quadrant). Each circle corresponds to a different site, and its radius is proportional to the local density. In panels a) and b), μ has been chosen such that particles at the trap center are in the CB phase. The density profile shows a cake-like structure, with concentric Mott-lobes with density $\rho = 1/2$ and $1/4$, analogous to the shells with contact interactions [2, 16]. We notice that in order to obtain a defect-free CB phase at the trap center

in panel (a) we had to perform temperature annealing of the system to remove the extended defects present in panel (b). These defects reflect the existence of a large number of low-energy metastable states, which are a direct consequence of the long-range nature of the interactions, and will be of relevance for experiments. In panel (c), μ has been chosen to realize an extended vacancy-SS region, surrounded by a SF. The density-distribution in the vacancy-SS looks similar to the CB phase. Panel (d) shows a disordered ST-phase at the center, surrounded by an extended Mott-shell with $\rho = 1/4$ (suggesting a less robust ST solid compared to CB and SR ones).

The phases above can be realized with polar molecules of current experimental interest, by tuning the depth of the confining optical lattices, or the strength of the DC field. For example, for RbCs ($d = 1.25$ Debye) with transverse and in-plane trapping $V_{0,\perp}/E_R = 40$ and $V_0/E_R = 4$, respectively, and lattice spacing $a = 400$ nm, $\omega_{\perp}/2\pi \gg \omega/2\pi > D/(a^3\hbar)$, with $D/(a^3\hbar) \simeq 3.5$ kHz, and thus the single-band Hamiltonian Eq. (1) is valid. With an in-plane tunneling rate $J/\hbar \simeq 120$ Hz, the ratio J/V can be tuned to any value $J/V \gtrsim 0.03$ by varying the strength of the DC field. We note that the Mott lobes of Fig. 1 will be also observed with fermionic molecules, e.g., KRb ($d = 0.5$ Debye) [6]. Since the interparticle distances can be larger than a μm , it may be possible to directly image the *spatial structure* of the Mott phases above using, e.g., tightly focused beams [22] (in alternative to Bragg scattering), while (small) coherence peaks should be visible in time-of-flight experiments in the superfluid phases.

Note added: While completing the present work, we became aware of a simultaneous, independent study on a *triangular* lattice with $\Omega = 0$, see Ref. [23].

The authors thank N. Prokof'ev, G. Astrakharchik, and the authors of Ref. [23] for fruitful discussions. This work was supported by ITAMP, MURI, the Austrian FWF, the EU through the STREP FP7-ICT-2007-C project NAME-QUAM, and the Spanish MEC (FIS2008-00784, QOIT).

-
- [1] I. Bloch, J. Dalibard, and W. Zwerger, *Rev. Mod. Phys.* **80**, 885 (2008).
 - [2] D. Jaksch *et al.*, *Phys. Rev. Lett.* **81**, 3108 (1998).
 - [3] M. Greiner *et al.*, *Nature (London)* **415**, 39 (2002); T. Stöferle *et al.*, *Phys. Rev. Lett.* **92**, 130403 (2004); S. Fölling *et al.*, *ibid.* **97**, 060403 (2006); I. B. Spielman, W. D. Phillips, and J. V. Porto, *ibid.* **98**, 080404 (2007); G.K. Campbell *et al.*, *Science* **313**, 649 (2006).
 - [4] F. Gerbier *et al.*, *Phys. Rev. Lett.* **101**, 155303 (2008); S. Trotzky *et al.* arXiv:0905.4882.
 - [5] See, e.g.: T. Lahaye *et al.*, arXiv:0905.0386.
 - [6] D. Wang *et al.*, *Phys. Rev. Lett.* **93**, 243005 (2004); J. M. Sage *et al.*, *ibid.* **94** 203001 (2005); T. Rieger *et al.*, *ibid.* **95** 173002 (2005); J. Deiglmayr *et al.*, *ibid.* **101**, 133004 (2008).

- (2008); S. D. Kraft *et al.*, J. Phys. B **39**, S993 (2006); K.-K. Ni *et al.*, Science **322**, 231 (2008); S. Ospelkaus *et al.*, Nat. Phys. **4**, 622 (2008); S. Y. T. van de Meerakker *et al.*, *ibid.* **4**, 595 (2008).
- [7] M. Baranov, Phys. Rep. **464**, 71 (2008); G. Pupillo *et al.*, arXiv:0805.1896, in *Cold Molecules: Theory, Experiment, Applications* (CRC Press, 2009); L.D. Carr *et al.*, arXiv:0904.3175.
- [8] H.P. Büchler *et al.*, Phys. Rev. Lett. **98**, 060404 (2007); A. Micheli *et al.*, Phys. Rev. A **76**, 043604 (2007).
- [9] H.P. Büchler, A. Micheli, and P. Zoller, Nat. Phys. **3**, 726-731 (2007).
- [10] N. V. Prokof'ev, B. V. Svistunov, and I. S. Tupitsyn, Phys. Lett. A **238**, 253 (1998); JETP **87**, 310 (1998).
- [11] An Ewald summation is used in the interaction potential.
- [12] J. Hubbard, Phys. Rev. B **17**, 494 (1978); M. E. Fisher and W. Selke, Phys. Rev. Lett. **44**, 1502 (1980); P. Bak and R. Bruinsma, *ibid.* **49**, 249 (1982).
- [13] M.P. Fisher *et al.*, Phys. Rev. B **40**, 546 (1989).
- [14] SS was found for [15]: *i*) *hard-core bosons* on a triangular lattice with nearest-neighbor (NN) interactions for $1/3 < \rho < 2/3$; *ii*) on a square lattice with NN and NNN interactions for $\rho < 0.25$ and $0.25 < \rho < 0.5$ between a "star" and a "stripe" solid at half filling; *iii*) *soft-core bosons* on a square lattice with NN and $\rho > 0.5$.
- [15] G. G. Batrouni *et al.*, Phys. Rev. Lett. **74**, 2527 (1995); P. Sengupta *et al.*, *ibid.* **94**, 207202 (2005); M. Boninsegni and N. Prokof'ev, *ibid.* **95**, 237204 (2005); S. Wessel and M. Troyer, *ibid.* **95**, 127205 (2005); L. Dang, M. Boninsegni and L. Pollet, Phys. Rev. B **78**, 132512 (2008).
- [16] G.G. Batrouni *et al.*, Phys. Rev. Lett. **89**, 117203 (2002).
- [17] F. J. Burnell *et al.*, arXiv:0901.4366
- [18] B. Capogrosso-Sansone, N. V. Prokof'ev, B. V. Svistunov, Phys. Rev. B **75**, 134302 (2007).
- [19] C. Menotti, C. Trefzger, and M. Lewenstein, Phys. Rev. Lett. **98**, 235301 (2007).
- [20] A.F. Andreev and I.M. Lifshitz, Sov. Phys. JETP **29**, 1107 (1969).
- [21] B. Spivak and S. A. Kivelson, Ann. Phys. **321**, 2071 (2006); T. Roscilde and J. I. Cirac, Phys. Rev. Lett. **98**, 190402 (2007) .
- [22] P. Würtz *et al.*, arXiv:0903.4837; J.I. Gillen *et al.*, arXiv:0812.3630.
- [23] L. Pollet, J. D. Picon, H. P. Büchler, and M. Troyer, to be submitted.